# Solid−Liquid Equilibria in an L-Isoleucine + L-Norleucine + Water System

**Toshimichi Kamei,*,† Kazuhiro Hasegawa,† Tatsuki Kashiwagi,‡ Eiichiro Suzuki,‡ Masaaki Yokota,§ Norihito Doki,§ and Kenji Shimizu§**

Isolation and Purification Technology Laboratory, Fermentation and Biotechnology Laboratories, Ajinomoto Company, Inc., 1-1 Suzuki-cho, Kawasaki-ku, Kawasaki-shi, 210-8681 Japan, Institute of Life Sciences, Ajinomoto Company, Inc., 1-1 Suzuki-cho, Kawasaki-ku, Kawasaki-shi, 210-8681 Japan, and Department of Chemical Engineering, Iwate University, 4-3-5 Ueda, Morioka, 020-8551 Japan

Solid−liquid equilibria in L-isoleucine (L-Ile) + L-norleucine (L-Nle) and water were measured at 293 K using the crystallization method. The L-Ile solubility in water is unaffected by small amounts of L-Nle. However, L-Ile solubility decreases rapidly with increased L-Nle. As for the solid phase, the formation of a solid solution of L-Ile and L-Nle was confirmed using synchrotron X-ray diffraction analysis.

## Introduction

L-Leucine (L-Leu), L-isoleucine (L-Ile), and L-valine (L-Val) are known as branched chain amino acids (BCAAs). They are essential amino acids used for intravenous feeding and as food additives. In most cases, they are commercially synthesized by fermentation. Small quantities of other amino acids including BCAAs are also synthesized as impurities in the processes where one BCAA is synthesized through fermentation. They are separated and purified by crystallization from fermentation broths containing impurities. During BCAA crystallization processing, guest amino acids (impurity amino acids) are readily incorporated into a host amino acid (a purified amino acid) because host and guest amino acids have similar branched hydrophobic side chains and crystal structures.[1−3] Molecular structures of these amino acids are shown in Figure 1.

In many cases, it is difficult to separate a host amino acid and guest amino acids from one another using a simple crystallization method such as cooling or concentration crystallization conducted in water. For that reason, repetition of recrystallization is necessary to purify BCAAs. To avoid this repetition and to obtain pure BCAAs efficiently, fundamental data such as solid−liquid equilibria in aqueous amino acid systems must be accumulated. Therefore, for this work, the L-Ile + L-Nle + water system was chosen as a model case.

## Experimental Section

***Chemicals.*** The L-Ile used in this experiment was obtained commercially (pharmaceutical grade) from Ajinomoto Co., Inc. (Tokyo, Japan), and L-Nle was supplied by Sigma-Aldrich Corp. (≥ 98 % (TLC)).

***Procedure.*** To confirm the solid−liquid equilibrium, the crystallization method was chosen in this experiment.

Crystallization experiments were conducted in a 1000 mL jacketed glass vessel at stirrer speeds of 300 rpm. At first, the L-Ile and L-Nle were added to the water. Then, the mixture of L-Ile, L-Nle, and water was heated to 80 °C and maintained at that temperature until the solution was dissolved completely.

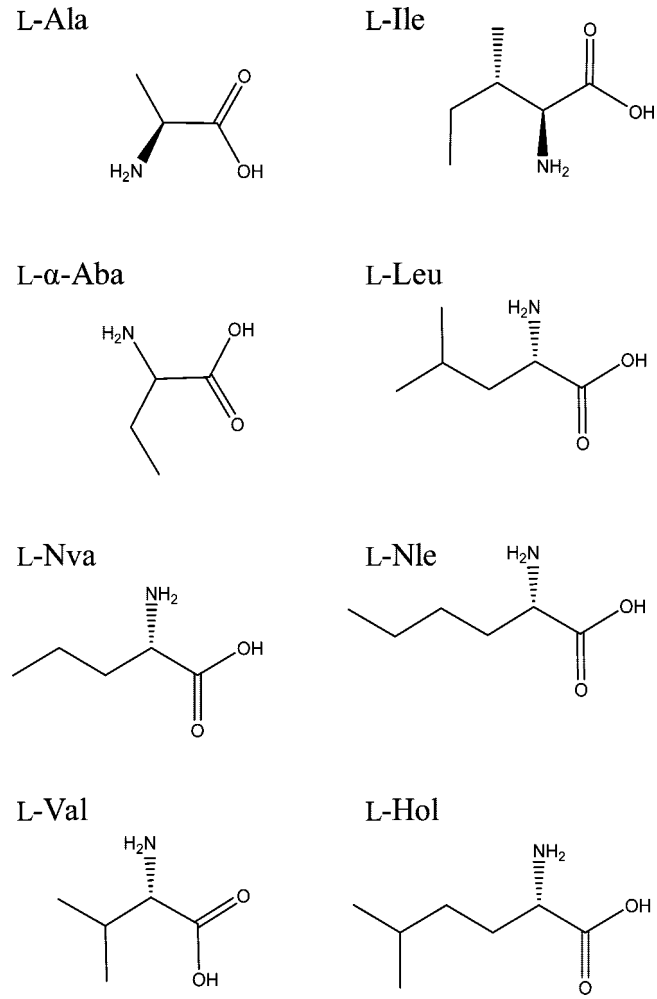


**Figure 1.** Molecular structures of BCAA and isomorphic amino acids.

The compositions of the starting solutions are presented in Table 1. After dissolution, the solution was placed in a jacketed glass vessel, and then the vessel was sealed. The temperature was controlled to (80 ± 0.1) °C using circulating water in the jacket from a programmable water bath. Subsequently, the solution was concentrated in a vacuum at 50 °C and crystallized. After

* Corresponding author. E-mail: toshimichi_kamei@ajinomoto.com.
† Fermentation and Biotechnology Laboratories, Ajinomoto Company, Inc.
‡ Institute of Life Sciences, Ajinomoto Company, Inc.
§ Iwate University.

10.1021/je800064n CCC: $40.75 
Published on Web 05/07/2008

**Table 1. Compositions of the Starting Solutions and Corresponding Phases in Equilibrium in the L-Ile (1) + L-Nle (2) + Water (3) System at 293 K**

| | initial | | equilibrium | | | |
|---|---|---|---|---|---|---|
| | liquid phase | | liquid phase | | solid phase | |
| run no. | $10^3\ x_1$ | $10^3\ x_2$ | $10^2\ x_1$ | $10^2\ x_2$ | $x_1$ | $x_2$ |
| Run 1 | 2.74 | 0.00 | 0.47 | 0.00 | 1.00 | 0.00 |
| Run 2 | 2.74 | 0.09 | 0.46 | 0.01 | 0.97 | 0.03 |
| Run 3 | 2.74 | 0.18 | 0.47 | 0.02 | 0.93 | 0.07 |
| Run 4 | 2.74 | 0.36 | 0.47 | 0.03 | 0.84 | 0.16 |
| Run 5 | 2.73 | 0.73 | 0.44 | 0.04 | 0.76 | 0.24 |
| Run 6 | 2.73 | 1.09 | 0.42 | 0.05 | 0.68 | 0.32 |
| Run 7 | 2.73 | 1.46 | 0.35 | 0.05 | 0.59 | 0.41 |
| Run 8 | 2.73 | 2.00 | 0.29 | 0.05 | 0.54 | 0.46 |
| Run 9 | 2.18 | 2.73 | 0.18 | 0.11 | 0.40 | 0.60 |
| Run10 | 1.09 | 2.73 | 0.09 | 0.15 | 0.25 | 0.75 |
| Run11 | 0.55 | 2.74 | 0.05 | 0.17 | 0.17 | 0.83 |
| Run12 | 0.18 | 2.74 | 0.02 | 0.18 | 0.08 | 0.92 |
| Run13 | 0.00 | 2.74 | 0.00 | 0.20 | 0.00 | 1.00 |

concentration, the concentrated slurry in the jacketed vessel was cooled rapidly to 20 °C using circulating water in the jacket. The temperature was then kept constant at 20 °C until no changes were observed in the liquid phase concentration. After achievement of steady state conditions, the contents of the vessel were filtered under a vacuum to collect the solid phase. After filtration, the obtained crystals were washed with 10 times the mass of acetone to remove adhesive impurities from the crystal surface. Finally, crystals were dried at room temperature.

The contents of L-Ile and L-Nle in the washed crystals and the saturated liquor (mother liquor) were analyzed using an amino acid analyzer (L-8800; Hitachi, Ltd.). The remaining solid samples were subjected to powder X-ray diffraction analysis (X′Pert-Pro-MPD; PANalytical B.V.) with a Cu Kα radiation source (wavelength = 1.54056 Å). They were also subjected to powder X-ray diffraction analysis using synchrotron radiation at the Pharmaceutical Industry Beamline BL32B2 of SPring-8. For measurements at SPring-8, powder samples were packed in glass capillaries, and their diffraction data were collected in the transmission geometry. The wavelength of the synchrotron radiation was set to 1.0000 Å. Diffraction images were recorded on the Imaging-Plate detector, R-AXIS V (Rigaku Corp.), and processed with a computer program (DisplayWin; Rigaku Corp.).

## Results

The measured liquid compositions and solid compositions for the mixture L-Ile (1) + L-Nle (2) + water (3) are listed in Table 1 and presented graphically in Figure 2.

Table 1 also lists the initial L-Ile mole fraction $x_1$ and L-Nle mole fraction $x_2$. The run number identifies the specific experiment. For example, in Run 2, a homogeneous aqueous solution containing $x_1 = 2.74 \cdot 10^{-3}$ and $x_2 = 0.09 \cdot 10^{-3}$ was concentrated and cooled to obtain a liquid phase containing $x_1 = 0.46 \cdot 10^{-2}$ and $x_2 = 0.01 \cdot 10^{-2}$, in equilibrium with a solid phase containing $x_1 = 0.97$ and $x_2 = 0.03$. Pure L-Ile and pure L-Nle crystallization were conducted, respectively, in Run 1 and Run 13.

As portrayed in Table 1 and Figure 2, from Run 2 to Run 4, the L-Ile solubility was not affected by the presence of a small amount of L-Nle. However, the L-Ile solubility decreases rapidly with increased mole fraction of L-Nle. The composition of the liquid phase would remain constant if the solid phase was a mixture of pure L-Ile and pure L-Nle. Consequently, the possibility exists that the solid phase is not a mixture of pure L-Ile and pure L-Nle but a solid solution is formed.

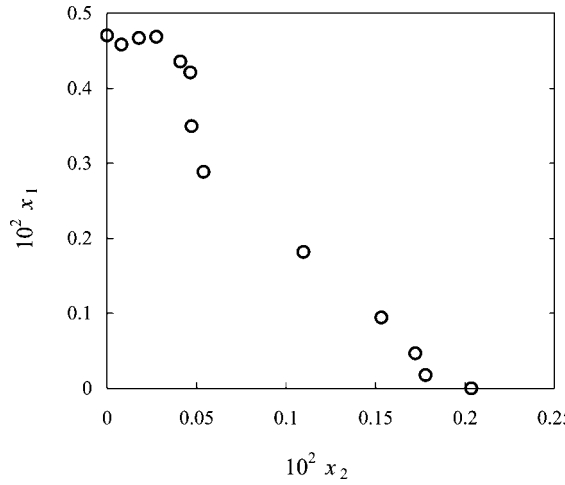


**Figure 2.** Ternary phase diagram for L-Ile (1) + L-Nle (2) + water (3). ○, Liquid-phase composition.

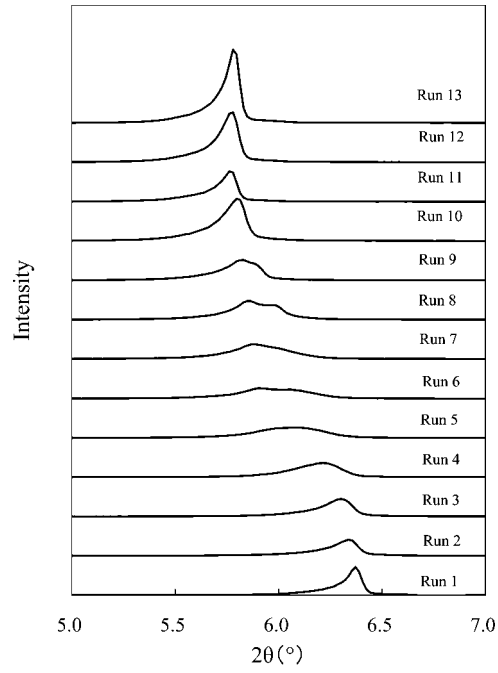


**Figure 3.** Powder XRD patterns of L-Ile + L-Nle crystals obtained from experiments using X'Pert-Pro-MPD (PANalytical B.V.) equipped with a Cu Kα radiation source (wavelength = 1.54056 Å).

**Table 2. Unit Cell Constants from Single-Crystal XRD Data**

| | lattice constant/Å | | |
|---|---|---|---|
| amino acid | *a* | *b* | *c* |
| L-Ile | 9.75 | 5.32 | 14.12 |
| L-Nle | 9.55 | 5.26 | 15.38 |

Figure 3 shows powder XRD diffraction patterns of crystals obtained in the experiments using X′Pert-Pro-MPD (PANalytical B.V.) with a Cu Kα radiation source (wavelength = 1.54056 Å). Actually, L-Ile is monoclinic and belongs to the $P2_1$ space group. In addition, the first peak in the powder XRD pattern corresponds to the (001) face, or the *c*-axis, of the unit cell. The lattice constants of L-Ile and L-Nle are shown in Table 2.[3,4] The crystal structures of L-Ile and L-Nle are similar except for the lengths of their *c*-axes. Therefore, the positions of the first peaks in their XRD patterns are useful to identify these amino acids.

The position and calculated *d*-spacing of the peaks are listed in Table 3. As the L-Nle composition in the solid phase

**Table 3. XRD Data and Calculated *d*-Spacing of Crystals of L-Ile (1) + L-Nle (2) Obtained in the Experiments Using X'Pert-Pro-MPD (PANalytical B.V.) Equipped with a Cu Kα Radiation Source (Wavelength = 1.54056 Å) versus Mole Fraction of the Solid Phase**

| | peak position | *d*-spacing | solid phase | solid phase |
|---|---|---|---|---|
| run no. | (2$\theta$) | *d*/Å | $x_1$ | $x_2$ |
| Run 1 | 6.37 | 13.86 | 1.00 | 0.00 |
| Run 2 | 6.34 | 13.94 | 0.97 | 0.03 |
| Run 3 | 6.30 | 14.01 | 0.93 | 0.07 |
| Run 4 | 6.21 | 14.21 | 0.84 | 0.16 |
| Run 5 | 6.09 | 14.49 | 0.76 | 0.24 |
| Run 6 | 5.90 | 14.96 | 0.68 | 0.32 |
| | 6.06 | 14.58 | | |
| Run 7 | 5.88 | 15.01 | 0.59 | 0.41 |
| Run 8 | 5.85 | 15.10 | 0.54 | 0.46 |
| | 5.97 | 14.79 | | |
| Run 9 | 5.83 | 15.14 | 0.40 | 0.60 |
| Run10 | 5.80 | 15.23 | 0.25 | 0.75 |
| Run11 | 5.76 | 15.33 | 0.17 | 0.83 |
| Run12 | 5.78 | 15.28 | 0.08 | 0.92 |
| Run13 | 5.78 | 15.28 | 0.00 | 1.00 |

increases, the XRD peak in the (001) face of L-Ile is shifted to the low-angle side. The XRD patterns were not obtainable using the patterns for the pure L-Ile (Run 1) and L-Nle (Run 13). These results confirm that L-Ile and L-Nle form a solid solution. However, when the L-Nle composition increases, these peaks broaden. It is therefore difficult to specify the peak positions, especially in Runs 2 to 9. The XRD diffraction patterns using synchrotron X-ray diffraction analysis (wavelength = 1.00 Å) were obtained using this potent X-ray source.

As portrayed in Figure 4, the images of (001) peaks in Runs 2 to 9 are sharper when using synchrotron X-ray diffraction analysis. A shoulder peak is confirmed from Run 5 to Run 9, and (001) peaks are obviously divided into two peaks, especially in Runs 6 and 8. This shoulder or division implies some different phases whose lattice constants are different in the solid solution.

The solid solution is probably formed by the substitution of the L-Ile molecule and the L-Nle molecule in the unit lattice. To explain the substitution of the L-Ile molecule and the L-Nle molecule in the unit lattice, the *c*-axis length in the solid solutions is calculated according to Vegard's law, and then the

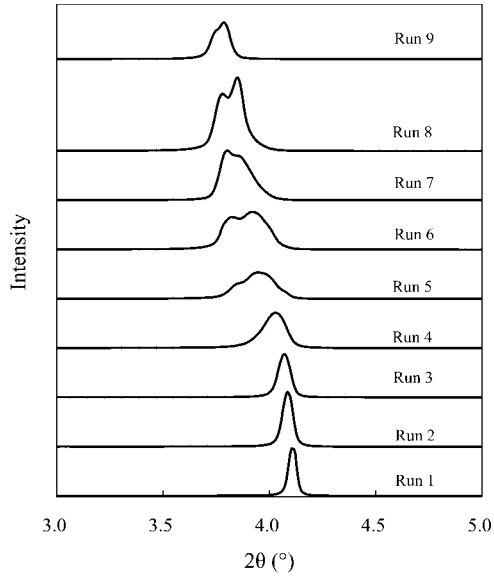


**Figure 4.** Powder XRD patterns of L-Ile + L-Nle crystals obtained in the experiments using synchrotron X-ray diffraction analysis (wavelength = 1.00 Å).

**Table 4. XRD Data and Calculated *d*-Spacing of Crystals of L-Ile (1) + L-Nle (2) Obtained in the Experiments Using Synchrotron X-Ray Diffraction Analysis (Wavelength = 1.00 Å)**

| | peak position | *d*-spacing | solid phase | obsd *c*-axis | calcd *c*-axis |
|---|---|---|---|---|---|
| run no. | (2$\theta$) | *d*/Å | $x_1$ | Å | Å |
| Run 1 | 4.11 | 13.94 | 1.00 | 13.94 | 13.94 |
| Run 2 | 4.09 | 14.03 | 0.97 | 14.03 | 13.98 |
| Run 3 | 4.07 | 14.09 | 0.93 | 14.09 | 14.05 |
| Run 4 | 4.03 | 14.21 | 0.84 | 14.21 | 14.17 |
| Run 5 | 3.95 | 14.52 | 0.76 | 14.52 | 14.32 |
| Run 6 | 3.82 | 14.99 | 0.68 | 14.63 | 14.41 |
| | 3.92 | 14.63 | 0.68 | 14.99 | 14.41 |
| Run 7 | 3.80 | 15.06 | 0.59 | 15.06 | 14.53 |
| Run 8 | 3.78 | 15.16 | 0.54 | 14.88 | 14.61 |
| | 3.85 | 14.88 | 0.54 | 15.16 | 14.61 |
| Run 9 | 3.79 | 15.14 | 0.40 | 15.14 | 14.81 |
| Run10 | 3.74 | 15.31 | 0.25 | 15.31 | 15.02 |
| Run11 | 3.72 | 15.40 | 0.17 | 15.40 | 15.13 |
| Run12 | 3.74 | 15.33 | 0.08 | 15.33 | 15.26 |
| Run13 | 3.73 | 15.38 | 0.00 | 15.38 | 15.38 |

calculated value and the observed value are compared. Vegard's law shows that the lattice length of the solid solution is related directly to the contents of substitution substances. [5] In this case, the length of the *c*-axis ($C_{calcd}$) is

$$C_{calcd} = C_{Ile} \cdot (1 - A) + C_{Nle} \cdot A \quad (1)$$

Therein, $C_{Ile}$ denotes the length of the *c*-axis of L-Ile; $C_{Nle}$ is the length of the *c*-axis of L-Nle; and *A* is a L-Nle mole fraction in the crystal. As a result, observed values show good agreement with calculated values in Runs 2 to 5 and in Runs 9 to 12. However, in Runs 6 and 8, where the (001) peaks are divided into two, observed values differ from the calculated values (Table 4, Figure 5). Therefore, as for the solid phase, the existing states of solid solutions are considered as follows.

L-Ile and L-Nle form a solid solution uniformly when the composition of L-Ile in the solid phase is large. Moreover, the lattice length is proportional to the amount of the substitution of L-Nle (in Run 2 to Run 5). On the other hand, when $x_1$ is from 0.55 to 0.70 in the solid phase, the solid solution is a mixture of some different phases whose lattice constants are different (Run 6 to Run 8). Actually, L-Ile and L-Nle form the solid solution uniformly when the composition of L-Nle in the solid phase is large. In addition, the lattice

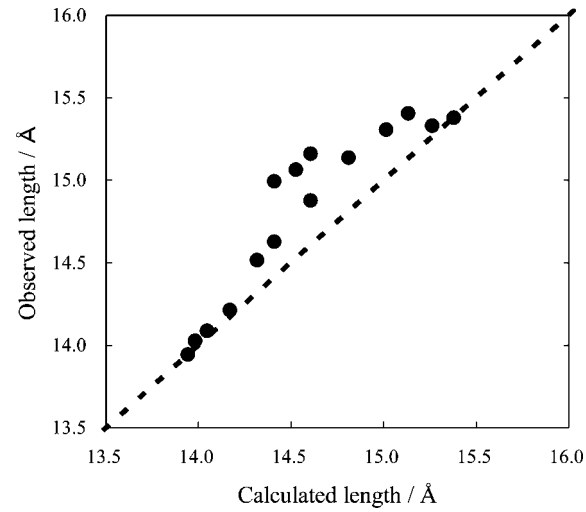


**Figure 5.** Relations between the calculated length of the *c*-axis and observed length of the *c*-axis. ●, observed value; dashed line, calculated value.

length is proportional to the amount of the substitution of L-Ile (Run 9 to Run 12).

## Conclusions

The solubility of L-Ile is not affected significantly when L-Nle is present in small quantities. However, it decreases rapidly with the addition of L-Nle. Moreover, as for the solid phase, when the composition of L-Ile or L-Nle in the solid phase is large, L-Ile and L-Nle form the solid solution uniformly. In addition, the lattice length is proportional to the amount of the substitution of L-Ile or L-Nle. On the other hand, when $x_1$ in the solid phase is 0.55 to 0.70, the solid solution is the mixture of some different phases whose lattice constants are different.

## Literature Cited

(1) Harding, M. M.; Howieson, R. M. L-Leucine. *Acta Crystallogr. B* **1976**, *32*, 633–634.
(2) Torii, K.; Iitaka, Y. The Crystal Structure of L-Valine. *Acta Crystallogr. B* **1970**, *26*, 1317–1326.
(3) Torii, K.; Iitaka, Y. The Crystal Structure of L-Isoleucine. *Acta Crystallogr. B* **1971**, *27*, 2237–2246.
(4) Torii, K.; Iitaka, Y. Crystal Structures and Molecular Conformations of L-Methionie and L-Norleucine. *Acta Crystallogr. B* **1973**, *29*, 2799–2807.
(5) Katoh, M. *X-ray diffraction analysis*, 5th ed.; Uchida Rokakuho: Tokyo, 1999; p 217.

Received for review January 28, 2008. Accepted March 27, 2008.

JE800064N